SOURCE PROVENANCE OF OBSIDIAN ARTIFACTS FROM LAS CAPAS, AZ AA:12:111 (ASM)

M. Steven Shackley
University of California, Berkeley

BERKELEY ARCHAEOLOGICAL
XRF LAB

Department of Anthropology
232 Kroeber Hall
University of California
Berkeley, CA 94720-3710

SOURCE PROVENANCE OF OBSIDIAN ARTIFACTS FROM LAS CAPAS (AZ AA:12:111 ASM) AND LOS POZOS (AZ AA:12:91 ASM), TUCSON BASIN, ARIZONA

by

M. Steven Shackley
Professor and Director
Archaeological XRF Laboratory
University of California, Berkeley

Report Prepared for

Desert Archaeology, Inc.
Tucson, Arizona

17 May 2011

INTRODUCTION

The analysis here of obsidian from these two San Pedro and Cienega Phase Early Agricultural period sites in the Tucson Basin is quite diverse including sources from the Sonoran Desert, and the eastern Arizona/western New Mexico region.

LABORATORY SAMPLING, ANALYSIS AND INSTRUMENTATION

All archaeological samples are analyzed whole. The results presented here are quantitative in that they are derived from "filtered" intensity values ratioed to the appropriate x-ray continuum regions through a least squares fitting formula rather than plotting the proportions of the net intensities in a ternary system (McCarthy and Schamber 1981; Schamber 1977). Or more essentially, these data through the analysis of international rock standards, allow for inter-instrument comparison with a predictable degree of certainty (Hampel 1984; Shackley 2011).

All analyses for this study were conducted on a ThermoScientific *Quant'X* EDXRF spectrometer, located in the Archaeological XRF Laboratory, El Cerrito, California. It is equipped with a thermoelectrically Peltier cooled solid-state Si(Li) X-ray detector, with a 50 kV, 50 W, ultra-high-flux end window bremsstrahlung, Rh target X-ray tube and a 76 µm (3 mil) beryllium (Be) window (air cooled), that runs on a power supply operating 4-50 kV/0.02-1.0 mA at 0.02 increments. The spectrometer is equipped with a 200 l min^{-1} Edwards vacuum pump, allowing for the analysis of lower-atomic-weight elements between sodium (Na) and titanium (Ti). Data acquisition is accomplished with a pulse processor and an analogue-to-digital converter. Elemental composition is identified with digital filter background removal, least squares empirical peak deconvolution, gross peak intensities and net peak intensities above background.

The analysis for mid Zb condition elements Ti-Nb, Pb, Th, the x-ray tube is operated at 30 kV, using a 0.05 mm (medium) Pd primary beam filter in an air path at 200 seconds livetime to generate x-ray intensity Ka-line data for elements titanium (Ti), manganese (Mn), iron (as $Fe_2O_3^T$), cobalt (Co), nickel (Ni), copper, (Cu), zinc, (Zn), gallium (Ga), rubidium (Rb), strontium (Sr), yttrium (Y), zirconium (Zr), niobium (Nb), lead (Pb), and thorium (Th). Not all these elements are reported since their values in many volcanic rocks are very low. Trace element intensities were converted to concentration estimates by employing a least-squares calibration line ratioed to the Compton scatter established for each element from the analysis of international rock standards certified by the National Institute of Standards and Technology (NIST), the US. Geological Survey (USGS), Canadian Centre for Mineral and Energy Technology, and the Centre de Recherches Pétrographiques et Géochimiques in France (Govindaraju 1994). Line fitting is linear (XML) for all elements but Fe where a derivative fitting is used to improve the fit for iron and thus for all the other elements. When barium (Ba) is analyzed in the High Zb condition, the Rh tube is operated at 50 kV and up to 1.0 mA, ratioed to the bremsstrahlung region (see Davis 2011; Shackley 2010a). Further details concerning the petrological choice of these elements in Southwest obsidians is available in Shackley (1988, 1995, 2005; also Mahood and Stimac 1991; and Hughes and Smith 1993). Nineteen specific pressed powder standards are used for the best fit regression calibration for elements Ti-Nb, Pb, Th, and Ba, include G-2 (basalt), AGV-2 (andesite), GSP-2 (granodiorite), SY-2 (syenite), BHVO-2 (hawaiite), STM-1 (syenite), QLO-1 (quartz latite), RGM-1 (obsidian), W-2 (diabase), BIR-1 (basalt), SDC-1 (mica schist), TLM-1 (tonalite), SCO-1 (shale), NOD-A-1 and NOD-P-1 (manganese) all US Geological Survey standards, NIST-278 (obsidian), U.S. National Institute of Standards and Technology, BE-N (basalt) from the Centre de Recherches Pétrographiques et Géochimiques in France, and JR-1 and JR-2 (obsidian) from the Geological Survey of Japan (Govindaraju 1994).

The data from the WinTrace software were translated directly into Excel for Windows software for manipulation and on into SPSS for Windows for statistical analyses. In order to evaluate these quantitative determinations, machine data were compared to measurements of known standards during each run. RGM-1 a USGS obsidian standard is analyzed during each sample run for obsidian artifacts to check machine calibration (Table 1). Source assignments were made by reference to Shackley (1995, 1998, 2005; see Table 1 and Figure 1 here), as well as source standard data at this lab.

DISCUSSION

Obsidian artifacts are relatively rare in Cienega Phase sites, although relatively common in the San Pedro Phase of the Early Agricultural (Shackley 2005). The obsidian provenance assemblage is similar to an earlier study at Las Capas that in that case was dominated by Sauceda Mountains obsidian (Shackley et al. 2003). The assemblage is quite diverse from Las Capas with sources from nearly all cardinal directions including Tank Mountains in the western Sonoran Desert in Yuma County, the Maricopa County sources of Sauceda Mountains and Sand Tanks, and the eastern Arizona/western New Mexico Antelope Creek source at Mule Creek (also available in the Gila River alluvium in the Safford Valley (Shackley 1992, 2005). Interestingly, the one Cienega Phase, Cienega projectile point from Los Pozos was produced from the Los Vidrios source along the Rio Sonoyta in northern Sonora to the southwest. The assemblage from both sites, taken as a whole, indicates the typical pattern of great diversity in the source provenance a likely result of contact and travel throughout the southern Southwest during the Early Agricultural Phases (Shackley 2005).

REFERENCES CITED

Davis, M.K., T.L. Jackson, M.S. Shackley, T. Teague, and J. Hampel
2011 Factors Affecting the Energy-Dispersive X-Ray Fluorescence (EDXRF) Analysis of Archaeological Obsidian. In *X-Ray Fluorescence Spectrometry (XRF) in Geoarchaeology*, edited by M.S. Shackley, pp. 45-64. Springer, New York.

Govindaraju, K.
1994 1994 Compilation of Working Values and Sample Description for 383 Geostandards. *Geostandards Newsletter* 18 (special issue).

Hampel, Joachim H.
1984 Technical Considerations in X-ray Fluorescence Analysis of Obsidian. In *Obsidian Studies in the Great Basin*, edited by R.E. Hughes, pp. 21-25. Contributions of the University of California Archaeological Research Facility 45. Berkeley.

Hildreth, W.
1981 Gradients in Silicic Magma Chambers: Implications for Lithospheric Magmatism. *Journal of Geophysical Research* 86:10153-10192.

Hughes, Richard E., and Robert L. Smith
1993 Archaeology, Geology, and Geochemistry in Obsidian Provenance Studies. *In Scale on Archaeological and Geoscientific Perspectives*, edited by J.K. Stein and A.R. Linse, pp. 79-91. Geological Society of America Special Paper 283.

Mahood, Gail A., and James A. Stimac
1991 Trace-Element Partitioning in Pantellerites and Trachytes. *Geochemica et Cosmochimica Acta* 54:2257-2276.

McCarthy, J.J., and F.H. Schamber
1981 Least-Squares Fit with Digital Filter: A Status Report. In *Energy Dispersive X-ray Spectrometry*, edited by K.F.J. Heinrich, D.E. Newbury, R.L. Myklebust, and C.E. Fiori, pp. 273-296. National Bureau of Standards Special Publication 604, Washington, D.C.

Schamber, F.H.
1977 A Modification of the Linear Least-Squares Fitting Method which Provides Continuum Suppression. In *X-ray Fluorescence Analysis of Environmental Samples*, edited by T.G. Dzubay, pp. 241-257. Ann Arbor Science Publishers.

Shackley, M. Steven
1988 Sources of Archaeological Obsidian in the Southwest: An Archaeological, Petrological, and Geochemical Study. *American Antiquity* 53(4):752-772.

1990 *Early Hunter-Gatherer Procurement Ranges in the Southwest: Evidence from Obsidian Geochemistry and Lithic Technology*. Ph.D. dissertation, Arizona State University, Tempe.

1992 The Upper Gila River Gravels as an Archaeological Obsidian Source Region: Implications for Models of Exchange and Interaction. *Geoarchaeology* 7:315-326.

1995 Sources of Archaeological Obsidian in the Greater American Southwest: An Update and Quantitative Analysis. *American Antiquity* 60(3):531-551.

1998 Intrasource Chemical Variability and Secondary Depositional Processes: Lessons from the American Southwest. In *Archaeological Obsidian Studies: Method and Theory*, edited by M.S. Shackley, pp. 83-102. Advances in Archaeological and Museum Science 3. Springer Publishing/Plenum Press, New York.

2005 *Obsidian: Geology and Archaeology in the North American Southwest*. University of Arizona Press, Tucson.

2011 An Introduction to X-Ray Fluorescence (XRF) Analysis in Archaeology. In *X-Ray Fluorescence Spectrometry (XRF) in Geoarchaeology*, edited by M.S. Shackley, pp. 7-44. Springer, New York.

Shackley, M.S., J.Kahn, E. Eklund, and C. Ogasawara
2003 Source Provenance of Obsidian Artifacts from San Pedro Phase through Protohistoric Contexts in the Tucson Basin, Arizona. Report prepared for Desert Archaeology, Inc., Tucson, Arizona.

Table 1. Elemental concentrations and source assignments for the archaeological specimens. All measurements in parts per million (ppm).

Sample	Ti	Mn	Fe	Rb	Sr	Y	Zr	Nb	Source
Las Capas									
12442	1001	549	8319	132	24	24	95	29	Superior (Picketpost Mtn)
780005	936	477	7860	119	20	22	93	26	Superior (Picketpost Mtn)
11102	960	395	10174	248	22	39	105	28	Antelope Cr (Mule Cr)
14655	931	382	9986	250	20	38	114	27	Antelope Cr (Mule Cr)
14605	1668	409	11429	174	79	35	206	26	Sauceda Mtns
2654	1114	544	11143	169	17	42	256	32	Sand Tanks
7543	1140	532	11035	166	12	39	251	31	Sand Tanks
12814	1155	416	10326	250	20	39	108	28	Antelope Cr (Mule Cr)
7994	1210	393	9170	171	150	20	126	17	Tank Mtns
Los Pozos									
2156	1030	260	11840	241	14	69	216	26	Los Vidrios
standard									
RGM1-S4	1591	291	13125	147	107	24	217	5	standard

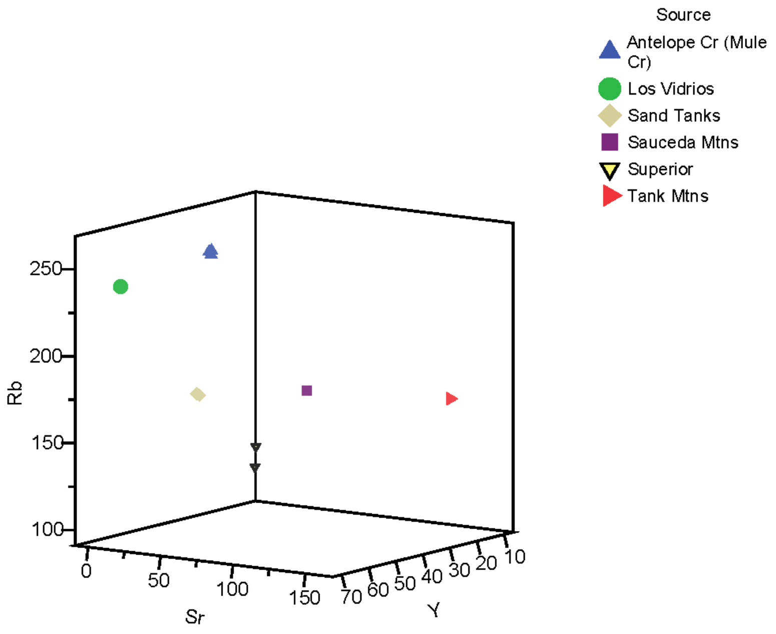

Figure 1. Sr, Rb, Y three-dimensional plot of the archaeological specimens.